DEPARTMENT OF SCIENTIFIC AND INDUSTRIAL RESEARCH

AND

FIRE OFFICES' COMMITTEE

JOINT FIRE RESEARCH ORGANIZATION

FIRE RESEARCH NOTE

NO. 537

FIRE SPREAD IN WOODEN CRIBS

by

P. H. THOMAS, D. L. SIMMS, AND H. G. H. WRAIGHT

February 1964.

Fire Research Station.
Boreham Wood.
Herts.
('phone ELStree 1341)

F.R. Note 537.

DEPARTMENT OF SCIENTIFIC AND INDUSTRIAL RESEARCH AND FIRE OFFICES' COMMITTEE
JOINT FIRE RESEARCH ORGANIZATION

FIRE SPREAD IN WOODEN CRIBS

by

P. H. Thomas, D. L. Simms and H. G. H. Wraight

SUMMARY

A theoretical model describing the steady spread of fire in cribs of wood in still air is shown to be in reasonable agreement with the results of laboratory experiments, the majority of which are by Fons and his colleagues. For a wide range of conditions the rate of fire spread R is given by $R\rho_b = 5\text{-}9$ mg cm^{-2} s^{-1} where R is in cm/s and ρ_b is the bulk density of the fuel bed.

FIRE SPREAD IN WOODEN CRIBS

by

P. H. Thomas, D. L. Simms and H. G. H. Wraight

1 - INTRODUCTION

This paper examines theoretically the problem of estimating how fast experimental fires spread along cribs of wood in still air. The physical aspects of the theory follow the lines described earlier by Fons[1] viz: every piece of fuel ahead of the fire receives heat from the burning zone and it is possible from a dynamic heat balance to relate rate of spread, geometrical and physical properties of the bed of fuel and variation of heat transfer with distance ahead of the fire front. The detailed formulation of the problem is, however, different from that given by Fons. Some general discussion of fire spread theory has also been published by Hottel et al[2].

2 - THEORY OF FIRE SPREAD

(a) Heating of fuel to ignition

The simplest expression for the steady state rate of spread in a continuous fuel bed can be derived on the following assumptions:-

(1) that heat losses ahead of the fire both from the base of the fuel bed to the ground and from the top of the bed to its surroundings can be neglected,

(2) that the material is inert and that its thermal properties do not vary prior to ignition; this has been shown to be adequate for the correlation of experimental data on ignition[3].

It follows from the existence of a steady state rate of burning that the ignition temperature, for any one fuel and one arrangement of crib, may be assumed to be constant. The rate of heat transfer to the fuel is then the rate at which it is brought to the ignition temperature multiplied by its thermal capacity of unit mass, i.e.

$$R \rho_b c \theta_o = i_o \qquad \ldots\ldots\ldots (1)$$

where R is the rate of fire spread

ρ_b is the bulk density of the fuel bed

c is the specific heat of the fuel

θ_o is the temperature rise above ambient to ignition

and i_o is the heat transfer rate per unit cross section of the fuel bed, perpendicular to the direction of fire spread.

If there is no heat transfer from the flames above the fuel bed and no convective transfer from within the burning zone, i_o is the radiation intensity from the burning zone.

Cooling losses from the fuel bed cannot necessarily be neglected, but by discussing the heat transfer through the fuel bed to a particular piece of fuel and considering its dynamic heat balance, an allowance can be made for them and this enables comparisons to be made between experimental results and theoretical predictions.

(b) Formulation of heat balance equations

Consider a long wide bed of fuel in which the burning zone is progressing in one direction at constant speed, see Fig.1, the fuel consisting of pieces having only one characteristic dimension, e.g. laminas of thickness 2a, square section sticks of side 2a, and cylinders or spheres of radius a. The intensity of heating around a piece of fuel whether by radiation or convection varies over the surface and differs for different positions of the fuel element with respect to the burning zone. If, for example, reflection and re-radiation are neglected, only the side nearer the fire receives radiation; for simplicity in what follows, no heat is assumed to flow parallel to a surface and each piece of fuel is assumed to be heated uniformly by a mean intensity chosen so that the total amount of heat received is the same as that actually received non-uniformly.

The mean rate of heating per unit surface area of fuel element can be described by

$$q'' = \sum_n I_n \, f_n(\alpha_n x) \qquad \ldots\ldots\ldots (2)$$

where f is an attenuation function yet to be specified

x is the distance ahead of the ignition front, this latter term being used to denote the position where the fuel reaches its ignition temperature

α_n is an attenuation coefficient

and I_n is a characteristic heat transfer rate, which is taken as the mean level around the whole of a fuel element which is just about to ignite.

From this definition it follows that

$$f_n(o) = 1 \qquad \ldots\ldots\ldots (3)$$

By postulating that there are several components of heating, the real function q'' may be regarded as the sum of several relatively simple

components. Thus there might be one function for radiation from the burning solid, one for radiation from the flames and another for convection.

During the spread of fire any one piece of fuel is heated from the ambient temperature up to the ignition temperature, (see p.1). Heat is lost at a rate $H\,\theta_s$ per unit area where θ_s is the instantaneous temperature rise and H is assumed constant for any stick size or crib design. The temperature rise of the surface of a piece of fuel may not reach θ_o until the flame front has actually passed. The distance between the ignition front, where the temperature rise is θ_o, and the flame front, where flames envelope the fuel, may be shown to be very small unless there is significant convective heating by flames.

Dimensional analysis and the linear relation between temperature rise and heat transfer show that the temperature of the surface at time λ will be described by an equation of the form

$$\theta_s = \sum_n \frac{I_n}{H} F_n \left(ha,\ h^2 k \lambda\right) \qquad \ldots\ldots\ldots (4)$$

where $h = H/K$ and $k = K/\rho c$

The functions F_n depend on the variation of the heating rate with time. In terms of a fixed distance co-ordinate x the variation of each component of heating with time is given by equation (2) with λ replaced by $x - R\lambda$ where R is the rate of spread, i.e.

$$q_n(\lambda) = I_n f_n\left[\alpha_n (x - R\lambda)\right] \qquad \ldots\ldots\ldots (5)$$

Thus, for a steadily moving system, in which λ cannot appear explicitly

$$H\,\theta_o = \sum I_n F^* \left(ha, \frac{h^2 k}{\alpha_n R}\right) \qquad \ldots\ldots\ldots (6)$$

where F^* is another unspecified function.

If the fuel is very thin, it warms up at an effectively uniform temperature throughout and the thermal conductivity may be regarded as infinite so that equation (6) must be of such a form that K does not appear in F^*, i.e. when $ha \to 0$

$$H\,\theta_o = \sum I_n P_n \left(\frac{H}{\rho c \alpha_n R}\right) \qquad \ldots\ldots\ldots (7i)$$

where P is a function as yet unspecified.

When the fuel element is thick enough for the inside to be effectively unheated when ignition takes place, equation (6) cannot involve a, i.e. when $ha \to \infty$.

$$H\,\theta_o = \sum I_n G_n \left(\frac{h^2 k}{\alpha_n R}\right) \qquad \ldots\ldots\ldots (7ii)$$

where G is a function as yet unspecified.

The next steps are to obtain expressions for the function F* and the particular forms P and G for any function f and later to evaluate these for two special forms evaluated for f.

(c) Evaluation of ignition equations

The surface temperature at time t due to an element of heat $q(\lambda)d\lambda$ striking unit area of surface at time t can be obtained by the methods described by Carslaw and Jaegar[4].

$$\delta\theta = \frac{2}{\rho c a} \sum_{n=1}^{\infty} \frac{(\gamma_n a)^2 e^{-k\gamma_n^2(t-\lambda)} q''(\lambda)d\lambda}{(ha)^2 + (\gamma_n a)^2 + h(ha)} \qquad \ldots\ldots (8)$$

where $h = 1$, 0 and -1 for a lamina, cylinder and sphere respectively.

For a lamina

$$(\gamma_n a)\tan(\gamma_n a) = ha \qquad \ldots\ldots\ldots (9)$$

for a cylinder

$$(\gamma_n a) J_1(\gamma_n a) = ha\ J_o(\gamma_n a) \qquad \ldots\ldots\ldots (10)$$

where J_o and J_1 are Bessel functions of the first kind of zero and first order respectively,

while for a sphere $(\gamma_n a)\cot(\gamma_n a) = 1 - ha$ ..... (11)

Equation (5) is inserted into equation (8), which is then integrated over $0 < \lambda < x'/R$. During this time θ rises from $\theta_{x'}$ to θ_o the temperature at the ignition front.

On putting x'/R equal to t and allowing this to tend to infinity, i.e. making the origin of the distance scale an infinite distance to the

left in Fig.(1), equation (8) reduces to

$$H\theta_o = 2\sum_n \frac{I_n H}{\rho c a R} \int_0^\infty \sum_{n=1}^{n=\infty} \frac{(\gamma_n a)^2 e^{-\frac{k\gamma_n^2 \phi}{R}} f_n(\alpha_n \phi)\, d\phi}{(ha)^2 + (\gamma_n a)^2 + h(ha)} \quad \ldots\ldots (12)$$

When $ha \to \infty$, thick fuels, the important part of the series consists of the higher terms $n > ha$ so that the series can be replaced by an integral (see Appendix) and equation (12) tends for all three values of h to

$$H\theta_o = 2\sum_n I_n \frac{H}{\rho c a R \pi} \int_0^\infty \frac{z^2\, dz}{(ha)^2 + z^2} \int_0^\infty e^{-\frac{kz^2\phi}{Ra^2}} f_n(\alpha_n \phi)\, d\phi \ \ldots$$

$$+ \frac{2H^2}{K \rho c R \pi} \sum_n I_n \int_0^\infty \frac{y^2\, dy}{y^2 + 1} \int_0^\infty e^{-\frac{k h^2 y^2 \phi}{R}} f_n(\alpha_n \phi)\, d\phi \quad \ldots\ldots (13)$$

When $ha \to 0$, thin fuels, only the first root of equations (9), (10) or (11) is required, the others giving terms which tend to zero. Equation (12) reduces to

$$H\theta_o = \sum I_n \frac{HM}{\rho c R a} \int_0^\infty e^{-\frac{M k h \phi}{R a}} f_n(\alpha_n \phi)\, d\phi \quad \ldots\ldots (14)$$

where $M = 1$, 2 and 3 for the lamina, cylinder and sphere respectively, all of which are seen to be the same if M/a is replaced by the ratio of surface to volume, i.e. S/V. It is therefore sometimes convenient to use the dimensionless group hV/S instead of ha.

(d) The attenuation functions

Fons[5] has pointed out that in still air the front of the burning zone remains vertical as it moves forward and he argues that this implies that radiation from the flames is negligible, since otherwise it would preferentially heat the upper part of the fuel bed, both ahead of the flame and in the crib itself. In conditions of no wind, cool air moves towards the burning zone so there is no sustained convection heating outside the flames. If some combustion products were deflected forward a little way, this too would tend to heat preferentially the upper part of the fuel bed.

If θ_o is defined as the temperature rise of the fuel just as it becomes enveloped in flames, convection transfer from the flames would have been excluded by definition though this would be at the expense of leaving the

value of θ_o uncertain. Alternatively, if θ_o is defined as the ignition temperature rise and convection is assumed constant within the flame, the component of convective heating would introduce

$$f_c(\alpha_c x) = 1 \quad \text{when} \quad 0 \leqslant x \leqslant \frac{1}{\alpha_c}$$

and $$f_c(\alpha_c x) = 0 \quad \text{when} \quad \frac{1}{\alpha_c} < x \qquad \ldots\ldots\ldots (15)$$

the suffix c denoting convection. $1/\alpha_c$ would be the distance between the plane at which the fuel ignites, (the ignition front) and the flame front itself, see Fig.(1). This distance is provisionally assumed negligible compared with the characteristic length for radiation transfer, and the present application of the theory to the experimental data is based on the assumption that convection is negligible and that the fuel surface temperature at the flame front is the ignition temperature. In extensions of this theory to other conditions, e.g. to include the effects of wind, allowance will have to be made for convection terms.

A discussion of the radiation transfer from the burning zone to the fuel ahead of the fire requires an assumption about the form of the crib and as a first approximation the fuel bed is idealised as an infinite lattice, the pieces of which are proportional to 'a' in size, separated from each other by distances which, for simplicity, are assumed equal. A single dimension 'a' and a spacing ratio then describes the fuel bed. Two cases will be considered:-

(1) The radiation is propagated as a "single ray" in the direction of spread.

(2) All parts of one half of the lattice, which is assumed to be the burning zone, produce radiation which is propagated into the other half at all angles. This will be referred to as "multiple ray".

(e) Single ray attenuation

Let N denote the number of pieces of fuel per unit volume and A their cross-sectional area effective in attenuating radiation (extinction cross-section). The value of A will depend on the assumed orientation of the fuel elements and is discussed below.

If i is the local intensity of radiation across a unit area in a vertical plane perpendicular to the direction of spread and i_o the intensity emitted by the fuel zone the attenuation of the radiation is

given approximately by

$$\delta i = -N A i \delta x \qquad \ldots\ldots\ldots (16)$$

i.e. $$i = i_0 e^{-N A x}$$

It follows that

$$f(x) = e^{-N A x} \qquad \ldots\ldots (16i)$$

so that we take

$$\alpha = N A \qquad \ldots\ldots (16ii)$$

This elementary formulation is strictly valid only if $N A \delta x$ can be small while $\delta x \gg \sqrt{A}$, i.e. $N^{\frac{2}{3}} A$ must be small. Also $N^{\frac{1}{3}} x$, the number of "mean free paths" considered, must be large. These requirements are not met in the experimental cribs but it will be seen below from measurements of attenuation that this treatment of attenuation will serve for the purpose of this paper. Indeed for fine forest fuels the errors will be less than with small cribs of timber fuel. Inserting equations (16i) and (16ii) into equation (12) gives

$$H \theta_0 = 2I(ha) \sum_{n=1}^{\infty} \frac{(\gamma a)^2 \left[(\gamma a)^2 + \left(\frac{\alpha R a^2}{k}\right)\right]^{-1}}{(ha)^2 + (\gamma a)^2 + \frac{1}{2}(ha)} \qquad \ldots\ldots\ldots (17)$$

If $\frac{hV}{S} \to 0$ and $\frac{\alpha RV}{HS}$ remains finite it follows* from equation (14) that

$$\frac{\alpha RV}{HS} = \frac{I_s}{H \theta_0} - 1 \qquad \ldots\ldots\ldots (18)$$

the suffix s denoting the "single ray" model.
For $\frac{hV}{S} \to \infty$, (thick fuel)

$$\frac{\alpha R}{h^2 k} = \left(\frac{I_s}{H \theta_0} - 1\right)^2 \qquad \ldots\ldots\ldots (19)$$

---

*In the theoretical discussion that follows we shall write down equations as if radiation were the only significant form of heating. This is to avoid unnecessary complication. If radiation is only one component and not the whole of the heat transfer then θ_0 is correspondingly only a component and not the whole of the ignition temperature rise. This follows from the linearity of equation (2).

For intermediate values of $\frac{hV}{S}$ the solution must be evaluated numerically from equation (17). The calculations show that there is only a slight difference between cylinders and spheres and the results are shown combined in Fig.(2). These calculations give theoretical values of R for given values of $\frac{H\,\Theta_o}{I_s}$, $\frac{hV}{S}$, the thermal properties and α .

Because I_s in equations (18) and (19) represents the mean intensity around the fuel element it follows that

$$I_s\,S = i_o\,A \qquad \ldots\ldots\ldots (20i)$$

which gives for a lamina perpendicular to the direction of spread.

$$I_s = i_o/2 \qquad \ldots\ldots\ldots (20ii)$$

for a cylinder perpendicular to the direction of spread

$$I_s = i_o/\pi \qquad \ldots\ldots\ldots (20iii)$$

and for a sphere or a square sectioned stick perpendicular to the direction of spread

$$I_s = i_o/4 \qquad \ldots\ldots\ldots (20iv)$$

(f) Multiple ray attenuation

In text books on radiation transfer and in the Appendix it is shown that if the burning zone and the zone ahead of the fire front can be considered ideally as semi-infinite regions consisting of equally or randomly spaced spheres, the attenuation function is given by

$$f_m(\alpha x) = \int_0^\infty \sigma\,dr \int_{\alpha x}^\infty \frac{e^{-(u^2+\sigma^2)^{\frac{1}{2}}}\,du}{u^2+\sigma^2} \qquad \ldots\ldots\ldots (21i)$$

where the suffix m refers to the multiple ray model. α is defined by equation (16ii). Rearranging the order of integration, equation (21i) becomes

$$f_m(\alpha x) = e^{-\alpha x} + \alpha x\,E_i(-\alpha x) \qquad \ldots\ldots\ldots (21ii)$$

For a comparison between theoretical and measured values we also require the variation of the radiation in a vertical plane

$$f_{m,v}(\alpha x) = 2\int_0^\infty r\,dr \int_{\alpha x}^\infty \frac{u-\alpha x}{(u^2+r^2)^{3/2}}\, e^{-(u^2+r^2)^{\frac{1}{2}}}\, du \qquad \ldots\ldots\ldots (22i)$$

the additional suffix v denoting the vertical component. $f_{m,v}$ has been normalised to unity at $x = 0$. It may readily be shown that

$$f_{m,v}(\alpha x) = e^{-\alpha x}(1-\alpha x) - (\alpha x)^2 E_i(-\alpha x)$$

$$= e^{-\alpha x} - (\alpha x) f_m(\alpha x) \qquad \ldots\ldots\ldots (22ii)$$

These theoretical expressions for f_m and $f_{m,v}$ in equations (21ii) and (22ii) respectively, are shown in Fig.3, together with the exponential form for equation (16i).

The total radiation received can never exceed half what would be received inside the burning zone, so that the maximum value of the average over all the surface of a fuel element is given by

$$I_m = i_o/2 \qquad \ldots\ldots\ldots (23)$$

Equation (12) must now be evaluated with f given by equation (21i).

It is shown in the Appendix that

$$\int_0^\infty e^{-q\phi} f_m(\alpha\phi)\, d\phi = \frac{1}{q} - \frac{\alpha}{q^2}\log_e\left(1+\frac{q}{\alpha}\right) \qquad \ldots\ldots\ldots (24)$$

with $q = k\gamma^2$. Equation (24) may be used to evaluate equation (12), which for spherical fuel elements and one component I becomes

$$\frac{H\theta_o}{I} = 2ha\sum_{r=1}^{\infty} \frac{1 - \frac{R\,a^2\alpha}{k\beta_r^2}\log_e\left(1+\frac{k\beta_r^2}{R\,a^2\alpha}\right)}{\beta_r^2 + (ha)^2 - ha} \qquad \ldots\ldots\ldots (25)$$

where $\beta_r \cot\beta_r = 1 - ha$

Instead of computing the series the following method was used to evaluate equation (25).

If ψ_m is $\frac{H\theta_o}{I}$ as given by equation (25)

ψ_s is $\frac{H\theta_o}{I}$ as given by equation (17) for a sphere

and $B = \frac{\alpha R\,a^2}{k}$

it may readily be shown that

$$B \frac{dy_m}{dB} + \psi_s = \psi_m \qquad \ldots\ldots\ldots (26)$$

Hence $$\psi_m = B \int_{\beta}^{\infty} \frac{\psi_s (b)\, db}{b^2} \qquad \ldots\ldots\ldots (27)$$

where b is a dummy variable for B

or $$\psi_m = B \int_{0}^{1/B} \psi_s (b)\, d (1/b) \qquad \ldots\ldots\ldots (28)$$

Equation (28) has been computed by graphical integration of the results in Fig.2 and the results are shown in Fig.4. It is shown in the Appendix that when $\frac{hV}{S} \to 0$ equation (25) becomes

$$1 - \frac{H \theta_o}{I_m} = \frac{1}{g} \log_e (1 + g) \qquad \ldots\ldots\ldots (29i)$$

where $$g = \frac{\mu S}{\rho_s C V \alpha R} \qquad \ldots\ldots\ldots (29ii)$$

and when $\frac{hV}{S} \to \infty$ equation (25) becomes

$$1 - \frac{H \theta_o}{I_m} = \frac{2}{j} \left[1 - \frac{1}{j} \log_e (1 + j) \right] \qquad \ldots\ldots\ldots (30i)$$

where $$j = \frac{H}{\sqrt{\alpha R K \rho C}} \qquad \ldots\ldots\ldots (30ii)$$

Equations (29i) and (30i) give the asymptotes which appear in Fig.(4).

(g) Comparison between the two models of attenuation

For the single ray model for spherical fuel elements equation (20iv) and equation (18) for $\frac{hV}{S} \ll 1$ and $\frac{H \theta_o}{I_s} \ll 1$ give

$$\frac{\rho_f C \alpha RV}{HS} \quad \text{or} \quad \frac{I_s}{H\theta_o} = \frac{i_o}{4 H \theta_o} \qquad \ldots\ldots\ldots (31)$$

For the multiple ray model, for $\frac{hV}{S} \ll 1$ and $\frac{H\,\theta_o}{I_m} \ll 1$, equations (23) and (29) give

$$\frac{2\,\rho_f\,C\alpha\,RV}{HS} \doteqdot \frac{I_m}{H\,\theta_o} = \frac{i_o}{2\,H\,\theta_o} \qquad \ldots\ldots\ldots (32)$$

and it is seen that the two models give the same relation between i_o and α for $\frac{hV}{S} \ll 1$.

When $\frac{H\,\theta_o}{I_s} \ll 1$ and $\frac{hV}{S} \gg 1$ equations (19) and (20iv) for the single ray model give

$$\sqrt{\frac{\alpha\,R}{h^2\,k}} = \frac{I_s}{H\,\theta_o} = \frac{i_o}{4\,H\,\theta_o} \qquad \ldots\ldots\ldots (33)$$

and for the multiple ray model, equations (23) and (30) give

$$\frac{3}{2}\sqrt{\frac{\alpha\,R}{h^2\,k}} = \frac{I_m}{H\,\theta_o} = \frac{i_o}{2\,H\,\theta_o} \qquad \ldots\ldots\ldots (34)$$

for this range of $\frac{hV}{S}$ and $\frac{H\,\theta_o}{I_s}$

The two models differ both in terms of I_m and i_o. For a given value of i_o there is 80 per cent difference in the two values of α ; for a given α , a 33 per cent difference in i_o.

(h) Expressions for α .

Consider first the single ray model and those pieces of fuel perpendicular to the direction of spread. For a crib of long square sticks or long cylinders of length L

$$A = 2\,a\,L \qquad \ldots\ldots\ldots (35)$$

The corresponding value of N is $1/(4\rho a^2 L)$, where ρ is the ratio of horizontal spacing between centres to stick size, i.e.

$$\alpha = \frac{1}{2\rho\,a} \qquad \ldots\ldots\ldots (36)$$

Inserting the apparent or bulk density ρ_b and the actual fuel density ρ_f for square sticks gives

$$\alpha = \frac{\rho_b}{2\,a\,\rho_f} \qquad \ldots\ldots\ldots (37)$$

For cylinders having their axes perpendicular to the direction of spread

$$\alpha = \frac{2 \rho_b}{\pi \rho_p a} \qquad \ldots\ldots\ldots (38)$$

and for spheres

$$\alpha = \frac{3 \rho_b}{4 \rho_p a} \qquad \ldots\ldots\ldots (39)$$

For the multiple ray theory the value of A should strictly be taken as the random projected area, i.e. the mean value of the projected area viewed from all angles. For a sphere this is obviously πa^2 both for a random fuel bed or an orientated one. For a fuel bed of cylinders or square section sticks it may also be shown to be one quarter of the surface area. That is, $\frac{\alpha a \rho_p}{\rho_b}$ is 0.50 for a square section stick and a cylinder, but 0.75 for a sphere. For all these and a lamina

$$\frac{\alpha V \rho_p}{S \rho_b} = \frac{1}{4} \qquad \ldots\ldots\ldots (40)$$

Equations (40) and (6) applied to one component of i_o lead to

$$\frac{R \rho_b C}{H} = F\left[\frac{H \theta_o}{i_o} , \frac{hV}{S}\right] \qquad \ldots\ldots\ldots (41)$$

In the notation used by Curry and Fons[6] $\sigma = S/V$ and λ is the volume of voids per unit surface area so that

$$\alpha = \frac{\sigma}{4(\lambda\sigma + 1)}$$

These results are summarised in Table 1.

Table 1

Theoretical values of $\frac{\alpha a \rho_p}{\rho_b}$

Shape	Single ray theory	Multiple ray theory
Square section	0.50	0.50
Cylinder	$\frac{2}{\pi} = 0.64$	0.50
Sphere	0.75	0.75

Equations (23), (29i) and (40) give

$$1 - \frac{2 H \theta_o}{i_o} = \frac{1}{g} \log_e (1 + g) \qquad \ldots\ldots (42i)$$

where $$g = \frac{4H}{R \rho_b C} \qquad \ldots\ldots (42ii)$$

as the theoretical equation for $\frac{hV}{S} \rightarrow 0$

As $g \rightarrow 0$ this reduces to

$$\frac{R \rho_b C \theta_o}{i_o} = 1 - 2.83 \frac{H \theta_o}{i_o} \qquad \ldots\ldots (42iii)$$

In principle, experimental measurements of the radiation received at various distances from a radiator inside a crib could be compared with the theoretical attenuation functions using the appropriate values of α from Table 1. However, in view of the limited accuracy required, a rather different comparison can be made and three possible ways are discussed below:-

(1) For small values of $\frac{H \theta_o}{I}$ and hence small values of $\frac{h^2 k}{\alpha R}$ the important property of the attenuation function, is the integral

$$\int_0^\infty f_m (\alpha \phi) \, d\phi \qquad \ldots\ldots (43)$$

and by analogy with the exponential function which appears in the single ray model the reciprocal of this integral serves to define α. In the Appendix it is shown that for the multiple ray theory

$$\int_0^\infty f_m (\alpha \phi) \, d\phi = \frac{1}{2\alpha} \qquad \ldots\ldots (44)$$

A value of α can therefore be obtained experimentally from half the reciprocal of the area under a curve of measured total attenuation.

(2) The radiation falling on a vertical surface, for example, a photocell is given by equation (22ii). If this is integrated over the whole range of x we obtain $2/3\alpha$, i.e. the radiation on a vertical surface is attenuated less rapidly than is the total radiation when both are normalised to unit value at the radiator. Thus an alternative estimate of α would be $\frac{2}{3}$ of the reciprocal of the area under the experimental $f_{m,v}$ curve.

(3) By analogy with the exponential function, one could obtain an attenuation coefficient from the slope at $x = 0$, but it can be shown from equation (21ii)

$$\left(\frac{d f_m}{dx}\right)_0 \longrightarrow -\alpha \qquad \ldots\ldots (45i)$$

On the other hand from equation (22ii)

$$\left(\frac{d f_v}{dx}\right)_0 = -2\alpha \qquad \ldots\ldots (45ii)$$

The theoretical framework relating R to the properties of the fuel bed is now in principle complete. It still remains to assign values to the various properties.

(i) Experimental determination of radiation attenuation

Radiant heat and light are both propagated according to the same geometric laws so that it is possible to use an optical analogue[7] to determine the attenuation of thermal radiation through a crib. Short lengths of cribs similar in cross-section to those used in experiments by Fons[8] and at the Joint Fire Research Organization[9] were constructed. Since unplaned wood has a high absorptivity[10] for the infra-red radiation from flames and may have a low one for the radiation from the tungsten filament lamps used as a light source, the wood sticks were painted black to minimise reflection of light. The radiation intensity was measured by the output from a photo-electric cell.

The variation in the intensity of radiation received over any given vertical plane in the crib parallel to the light source was small. This is in itself consistent with the result obtained by Fons with cribs of cross-sectional area at least as large as the ones used in these experiments, where the rate of spread is almost independent of the crib height and width.

Only a few measurements of attenuation were made, and they refer to:-

(a) the total radiation received on the vertical and horizontal faces of the sticks, Fig.5a,

(b) the radiation received on the vertical face only, Fig.5b.

Measurements could only be obtained in the "tail" of the distribution function but they show that its form is curved and more like f_m than f_v, see Fig. (3).

To obtain a best value for $\frac{\alpha a \rho_f}{\rho_b}$ the integrations referred to above were performed. In the "missing" part of the curve a straight line was assumed, i.e. an exponential form, and this has the effect of overestimating the area and hence underestimating the value of α. The results calculated this way are shown in Table 2. The results for the three values of ρ_b give similar values for $\frac{\alpha a \rho_f}{\rho_b}$ to those predicted theoretically.

Table 2

Experimental values of attenuation α - cm^{-1}

Stick thickness = 1.3 cm, (i.e. a = 0.65 cm)

$\frac{\rho_f}{\rho_b}$	Single ray		Multiple ray			
			Vertical component		Total radiation	
	cm^{-1}	$\frac{\alpha a \rho_f}{\rho_b}$	cm^{-1}	$\frac{\alpha a \rho_f}{\rho_b}$	cm^{-1}	$\frac{\alpha a \rho_f}{\rho_b}$
4	0.49	1.25	0.33	0.83	0.30	0.75
5	0.39	1.23	0.26	0.81	0.23	0.73
6	0.33	1.25	0.22	0.83	0.19	0.74
Mean values		1.25		0.83		0.74

The above values of α and $\frac{\alpha a \rho_f}{\rho_b}$ should strictly be reduced by the factor $\left(1 - \rho_b/2\rho_f\right)$, which has the values 0.88, 0.90 and 0.92 to allow for the obscuration of the radiation by the cross section of the sticks of wood parallel to the direction of fire spread. The mean ratios in Table 2 then become 1.10, 0.75 and 0.67 respectively.

The multiple ray theory gives better agreement with the theoretical result of 0.50 but the discrepancy between even this and the experimental value of 0.67 is about 30 per cent. The error arises from the very considerable difference between the actual crib construction and that assumed in the theoretical model. However, in spite of this, the fact that the value of $\frac{\alpha a \rho_f}{\rho_b}$ is virtually constant for a variation of 50 per cent in ρ_f/ρ_b, (even though the theory assumes that the spacing is equal in the vertical and horizontal directions), means that the agreement is sufficiently good for the purpose of this paper. The model may well be in greater error for these experimental cribs than for a more randomly arranged natural fuel bed.

3 - ANALYSIS OF EXPERIMENTAL DATA ON FIRE SPREAD

Most of the large number of experiments with cribs reported by Fons and his colleagues[8] are for white fir but some results for magnolia, basswood, sugar maple and longleaf pine are also given. Values of the steady rate of spread, R, were obtained for different densities of the same wood in cribs of sticks mostly 1.3 cm thick, spaced apart at a horizontal distance which was 4 cm in the great majority of the experiments. Different widths and heights of crib were employed, but except for two tests with shallow cribs neither the width nor the height noticeably affects the rate of spread. This is in accordance with the preceding theory which relates R to the mass of fuel per unit volume. The cribs had moisture contents M ranging from 2.5 to 17 per cent by weight, and the preceding theory can take into account certain of its effects. The effective specific heat of the wet wood C_M can be evaluated from the heat required to raise wet wood to the ignition temperature, the heat of wetting[11] and the latent heat.

The temperature at which the water vapour leaves the fuel bed cannot be predicted and has been assumed to occur at 100°C.

Thus $$C_M \theta_o = C_o \theta_o + M . \Delta H + \Delta W \qquad \ldots\ldots\ldots (46)$$

where ΔH is the difference in enthalpy between vapour at 100°C and liquid at 20°C.

$C_o = 0.34$[12]

ΔW is the heat of wetting equal to 16 cal/g[13] and

$\theta_o \doteqdot 300°C$[14]

The variation of thermal conductivity with moisture content has been calculated by Maclean[15] and the density of the wet wood calculated from the method of mixtures.

Equation (41) states that the variables concerned can be combined into three groups only. Although these are given as

$$\frac{R \rho_b C_M}{H} \quad , \quad \frac{H \theta_o}{i_o} \quad \text{and} \quad \frac{hV}{S}$$

any three independent combinations of these may be used. H appears in all three variables above and it is not possible to obtain more than one variable which is independent of both H and i_o. This is $\frac{R \rho_b C_M V}{KS}$

and this variable is plotted against $\frac{hV}{S}$ for various values of $\frac{H\,\theta_o}{i_o}$ as calculated from single ray theory in Fig.6a (multiple ray in Fig.6b) with a similar plot of $\frac{R\,\rho_b\,C_M}{H}$ against $\frac{hV}{S}$ in Fig.7a (multiple ray in Fig.7b). A comparison between experiment and theory for various values of $\frac{H\,\theta_o}{i_o}$ then permits an estimate to be made of i_o for any value of H provided H is assumed constant.

H for an isolated stick varies slightly with stick size, the convective component varies as $(V/S)^{-\frac{1}{4}}$ and the radiation component, if present, is constant. The heat transfer from sticks directly above each other would depend weakly on the height of the crib and would be slightly less for the upper sticks. The same would also be true if the fuel bed were packed sufficiently tightly so that the bulk of the air as well as the boundary layer became heated. Such a variation of H with height would lead to the burning zone being inclined to the vertical and since this is not observed no allowance has been made for it. The bulk of Fons' data are for 1.3 cm sticks and a reduction to 0.7 cm or an increase to 3.2 cm leads to change either way by a factor of about 20 per cent for a purely convective loss.

The gradient of temperature along the crib is steep so that some radiation transfer will take place from hotter to cooler sticks. In view of these considerations, it is doubtful if any departure from a constant H need be considered in the analysis of experimental data.

No values of i_o are reported by Fons and the data have accordingly been analysed on the assumption that both H and $\frac{H\,\theta_o}{i_o}$ are constant. Values of $\frac{R\,\rho_b\,C_M}{H}$ and $\frac{hV}{S}$ were calculated from Fons' data assuming a value for H of 8×10^{-4} cal cm^{-2} s^{-1} deg C^{-1}, and are plotted in Fig.8a. The two tests referred to above where the burning rate was markedly lower than in similar tests with deeper cribs were excluded. The best curves derived from the single ray theory, Fig.2, and the multiple ray theory, Fig.4, are also shown in Fig.8a. The results are also plotted in Fig.8b using the alternative form of variables $\frac{R\,\rho_b\,C_M V}{KS}$ and $\frac{hV}{S}$ and are again compared with the theoretical curves.

The problem of evaluating H and its variation within fuel beds will be discussed in greater detail in a separate report, but Fig.9 shows how the estimate of i_o is affected by the choice of H.

A convenient measure of the position of the central cluster of experimental points in Fig.8a was taken as $\frac{R\,\rho_b\,C_M}{H} \sim 6.7$ and $\frac{hV}{S} \sim 0.8$ for the single ray curve, and, whatever value was assumed for H the curve having the best value of $\frac{H\,\theta_o}{I_s}$ would have to be fitted close to this point. Consequently the above numerical values can be altered for any arbitrary

change in H and the appropriate value of i_o obtained from Fig.7a. A similar procedure was adopted for the multiple ray curves. A change in H would, however, alter the shape of the curve passing through the main cluster of experimental data, but this would not be very apparent for the range of H shown in Fig.9. The estimate of i_o varies approximately as the square root of the value of H, which itself is unlikely to be outside the range 4 to 10 cal cm^{-2} s^{-1} deg C^{-1}. The uncertainties regarding H and the choice of theory make the estimate of i_o rather imprecise but 1 to 2 cal cm^{-2} s^{-1} is in the range to be expected for this mode of heat transfer.

4 - DISCUSSION

(1) For the value assumed for H, the comparison between single ray theory and experiment gives the best value for $\frac{H \theta_o}{i_o}$ as 0.12, θ_o is taken as the minimum temperature for ignition in the presence of a small flame[14], i.e. 300°C, and independent of species, so that the best value of i_o is estimated to be about 2.0 cal cm^{-2} s^{-1}. Taking a value for H of say 4×10^{-4} cal cm^{-2} s^{-1} deg C^{-1} would reduce the estimate of i_o to about 1.4 cal cm^{-1} s^{-1} for these data. These values are in the range expected, giving black body temperatures for the burning zone of about 800°C.

(2) The correlation is satisfactory not only because the estimated numerical value of i_o. (2.0 cal cm^{-2} s^{-1}) is a reasonable one but also because the experimental data lie about the theoretical relation in a region where the cribs can be regarded as neither thin nor thick in the thermal sense.

(3) A comparison between the data shown in Figs 8a and 8b and the two forms of the theory suggests that that based on single ray attenuation, which shows less curvature than that based on multiple ray, is the more satisfactory description of the experimental relation between the theoretically derived variables.

(4) Any tendency for H to decrease as the stick size increased would reduce the horizontal scale for the experimental data. If anything this would improve the agreement, and could even make the multiple ray theory better than the single ray theory, in which case the best value of i_o is somewhat lower, for $\frac{H \theta_o}{I_m}$ is 0.35 which gives i_o as about 1.4 cal cm^{-2} s^{-1}.

(5) From equations (18) and (40) the best theoretical line with $\frac{H \theta_o}{i_o}$ = 0.12 and a mean value for C_M of 0.6 cal g^{-1} deg C^{-1} gives a lower asymptotic limit for $R\rho_s$ of 6 mg cm^{-2} s^{-1}. Multiple ray theory gives a lower limit of about 4 mg cm^{-2} s^{-1}.

A statistical examination of the results for white fir shows that the upward trend with $\frac{hV}{S}$ is real and that there is little or no effect of moisture other than that accounted for in the term C_M.

5 - OTHER RESULTS FOR CRIBS AND FOREST FUELS

The following additional results are also plotted in Figs 8a and 8b:-

(i) Fons' results for four other species

(ii) J.F.R.O. results for spread in long cribs of 0.7, 1.3 and 2.5 cm thick sticks.

(iii) J.F.R.O. results for radial spread in cribs of 2.5 and 1.3 cm thick sticks with a spacing factor up to 8:1 and heights up to 120 cm.

These results which cover a relatively wide range of crib designs are more scattered but straddle the theoretical line. There is clearly some difference between the different species used by Fons which has not been accounted for in the present calculations but clearly the results show that in broad terms the theory gives variables which correlate a large part of the data and gives quantitative estimates of the right order. Experimental values of i_o are being obtained to provide a more detailed comparison between theory and experiment.

Curry[6] and Fons have given some results for radial spread in still air through sticks of various sizes and several species of pine needles in a randomised bed. Values of $\frac{V}{S}$ vary from 0.01 to 0.16 cm ($6 < \sigma < 100$ cm^{-1}). Except for wood wool shavings, which was the thinnest fuel used, the results, which will be discussed in more detail elsewhere, give values for $R\rho_b C_M \theta_o$ of order 0.8 to 1.7 cal cm^{-2} s^{-1}. This heating rate is consistent also with the main mechanism of heat transfer being the radiation from the fuel bed but the rate of spread varies with 'λ' the volume of voids per unit surface area, an effect in addition to its effect on bulk density, so that other factors are clearly involved.

For specific surfaces from 6 to 65cm^{-1} and values of 'λ' ranging from 0.13 to 0.90 cm the results for a moisture content of about 9 per cent can be expressed as $R\rho_b$ equal to 7 mg cm^{-2} s^{-1} ± 30 per cent. At a value of 'λ' corresponding to the cribs described here these data give $R\rho_b \simeq$ 5 mg cm^{-2}s^{-1}. This is in satisfactory agreement with the lower limit for thin sticks obtained from the crib data described in this report.

6 - CONCLUSIONS

(1) A theoretical model based on radiation transfer from the burning fuel though the fuel bed correlates a large number of results satisfactorily.

(2) The value of the radiation emitted from the burning zone may be estimated from the theory and this value is a realistic one.

(3) The mass burning rate, $R\rho_b$, of the crib in still air lies in the range 5 to 9 mg cm^{-2} s^{-1} and tends to approximately the same lower limit as that for beds of thin sticks and pine needles.

(4) The crib used by Fons and the Joint Fire Research Organization are too thick to represent thin fuels and too thin to represent very thick fuels.

7 - REFERENCES

(1) FONS, W. L. Analysis of Fire Spread in Light Forest Fuels. J. Agric. Res. (1946) 72 (3) 93-143.

(2) HOTTEL, H. C. et al. A study of fire problems. National Academy of Sciences, National Research Council, Washington, D.C. Publication 949-1961.

(3) SIMMS, D. L. Damage to cellulosic solids by thermal radiation. Combustion and Flame, 1962, 6, 4, 303-318.

(4) CARSLAW, H. S. and JAEGER, J. C. Conduction of heat in solids, Oxford University Press 1959, 2nd edition.

(5) FONS, W. L. Private communication.

(6) CURRY, J. R. and FONS, W. L. Forest fire behaviour studies. Mech. Eng. 1940, 62 (3), 219-225.

(7) LAWSON, D. I. and HIRD, D. A photometric method of determining configuration factors. Brit. J. Appl. Phys. 1954, 5 (2) 72-4.

(8) FONS, W. L., CLEMENTS, H. B., ELLIOTT, E. R. and GEORGE, P. M. Project fire model. Summary Progress Report II. Forest Service, U.S. Dept., Agriculture, Southern Forest Fire Laboratory, Macon, Georgia, 1962.

(9) THOMAS, P. H., SIMMS, D. L. and WRAIGHT, H. Some experiments on fire spread in wood cribs. Joint Fire Research Organization, F.R. Note in preparation.

(10) SIMMS, D. L., LAW, Margaret and HINKLEY, P. L. The effect of absorptivity on the ignition of materials by radiation. Joint Fire Research Organization F.R. Note 308/1957.

(11) HEARMON, R. F. S. and BURCHAM, J. N. Specific heat and heat of wetting of wood. Nature, 176, Nov.26 (55) 978.

(12) DUNLAP, F. The specific heat of wood. Forest Service Bulletin No.110. U.S. Dept. of Agrigulture, Washington, 1912.

(13) KRUYT, H. R. and MODDERMAN, J. G. Heats of adsorption and wetting. International Critical Tables. Vol.5, p.143.

(14) SIMMS, D. L. Surface spread of flame. Joint Fire Research Organization F.R. Note in preparation.

(15) MACLEAN, J. D. The thermal conductivity of wood. Trans. Amer. Soc. Heat. Vent. Engrs. 1941, 47, 1184.

APPENDIX

1. Radiation from cloud of particles.

By regarding a fuel bed as a cloud of absorbing particles the integral expressions for radiation transfer through absorbing gases or clouds of coal particles as given by Nusselt may be employed to calculate the attenuation.

Results are derived in this Appendix in terms of this idealisation of a fuel bed as an infinite medium of randomly spaced particles.

Let Q be the total radiation emitted by one particle
N be the number of particles per unit volume
A be the mean extinction cross-section of a particle to a narrow angle ray from any direction.
$x' y' z'$ be the co-ordinates of a small volume of radiators
and $x\ y\ z$ be the co-ordinates of the receiver

In volume $dx'dy'dz'$ there are $N\,dx'dy'dz'$ radiators and if the elementary volume is small enough there are sufficiently few radiators to neglect the obscuration of one by the others.

The total radiation passing from these if $NQ\,dx'dy'dz'$ and the radiation received by a particle at x, y, z.

is $$\frac{ANQ\,dx'dy'dz'e^{-NA\left[(x-x')^2+(y-y')^2+(z-z')^2\right]^{\frac{1}{2}}}}{4\pi\left[(x-x')^2+(y-y')^2+(z-z')^2\right]} \qquad (1.1)$$

If radiating particles are supposed to be confined to the region

$$-\infty < x' < 0,\quad -\infty < y' < \infty,\quad 0 < z' < H$$

and particles outside this region are receivers only (i.e. reradiation is neglected) it follows that the total radiation received by a single particle is

$$Q' = \frac{ANQ}{4\pi}\int_{-\infty}^{\infty}dy'\int_{0}^{H}dz'\int_{-\infty}^{0}dx'\,\frac{e^{-NA\left[(x-x')^2+(y-y')^2+(z-z')^2\right]^{\frac{1}{2}}}}{(x-x')^2+(y-y')^2+(z-z')^2} \qquad (1.1)$$

Clearly the maximum possible value for Q' would be obtained with a radiating region extending to infinity in all directions. The radiating particles are assumed to be in thermal equilibrium so that each particle receives Q and emits Q. Close to the edge of a large radiator a body receives half the heat it would receive away from the edge but this in turn is half what it would receive in a uniform field. Thus when Z is zero and the radiating region is semi-infinite

the value of Q tends to a maximum of $Q/4$. On the mid-plane the value of Q' is given by the same integral as above but with limits of $\pm H/2$ for z.

We normalise the radiation to unit value at $x = 0$ so that at any other position on a level with the centre at the radiating zone ($z = H/2$) the mean intensity of radiation relative to the maximum value at $x = 0$ is

$$\frac{4Q'}{Q} = f_m = \frac{AN}{\pi} \int_{-\infty}^{\infty} dy' \int_{0}^{H} dz' \int_{-\infty}^{0} dx' \frac{e^{-NAS}}{S^2} \tag{1.2}$$

where $S^2 = (x-x')^2 + (y-y')^2 + (z-z')^2$

and $y = z = 0$

and for a receiver on the mid-plane of $z = H/2$

$$\frac{2Q'}{Q} = f_m = \frac{AN}{2\pi} \int_{-\infty}^{\infty} dy' \int_{-H/2}^{H/2} dz' \int_{-\infty}^{0} dx' \frac{e^{-NAS}}{S^2} \tag{1.3}$$

It will be noticed that equation (1.3) for f_m is equal to equation (1.2) with H replaced by $H/2$. We shall therefore discuss

$$f_m = \frac{2}{\pi} \alpha \int_{0}^{\infty} dy' \int_{0}^{H} dz' \int_{-\infty}^{0} dx' \frac{e^{-\alpha S}}{S^2} \tag{1.4}$$

where $\alpha = AN$ and where the symmetry with respect to y' has been allowed for.

The radiation intensity is expressed by a maximum intensity at $x = 0$ of I and a distribution function $f(\alpha x)$ and I is <u>half</u> the value within the radiating cloud. That is if the particles were spheres of radius r, $Q/4\pi r^2$ is the maximum radiation intensity within the cloud system. This is denoted by $i_0 = 2I$, equation (23).

Let $\alpha(x-x') = u$, $\alpha y' = v$, $\alpha z' = w$ and $H/x = \Omega$

so that on replacing the original co-ordinates we have

$$f_m = \frac{2}{\pi} \int_{0}^{\infty} dv \int_{0}^{\alpha H} du \int_{\alpha x}^{\infty} dw \frac{e^{-(u^2 + v^2 + w^2)^{\frac{1}{2}}}}{u^2 + v^2 + w^2} \tag{1.5}$$

When $\alpha H \to \infty$, polar co-ordinates r , θ can be used in the v w planes and the integral becomes

$$f_m = \int_0^\infty r\,dr \int_{\alpha x}^\infty du \frac{e^{-(u^2 + r^2)^{\frac{1}{2}}}}{u^2 + r^2} \tag{1.6}$$

The radiation falling on the vertical yz plane is the same as that given by equations (1.2), (1.3), (1.4) and (1.5) except that the cosine of the angle at the receiver between the elementary volume and the x axis i.e. $(x - x')/S$ appears in the integrand. However, the maximum radiation falling on a vertical unit area is half that falling on a sphere and to normalise the radiation to unit value at $x = 0$ we need to include a factor of 2, i.e.

$$f_{m,v}(\alpha x) = \frac{4}{\pi}\int_0^\infty dv \int_0^{\alpha H} dw \int_{\alpha x}^\infty du \frac{u e^{-(u^2 + v^2 + w^2)^{\frac{1}{2}}}}{(u^2 + v^2 + w^2)^{3/2}} \tag{1.7}$$

when αH is infinite the integration in the v w plane is done in polar co-ordinates, i.e.

$$f_{m,v}(\alpha x) = 2\int_0^\infty r\,dr \int_{\alpha x}^\infty du \frac{u e^{-(u^2 + r^2)^{\frac{1}{2}}}}{(u^2 + r^2)^{3/2}}$$

2. The integration of the attenuation function.

In the course of evaluating the rate of spread due to such radiation transfer it becomes necessary, see equation (12), to evaluate

$$\psi = \int_0^\infty f_m(\alpha x) e^{-qx}\,dx \tag{1.8}$$

where q depends on the rate of spread and the thermal properties of the fuel ahead of the fire. Here we shall be concerned only to evaluate the integral.

The integration is straightforward if $\alpha H \to \infty$ in which case we replace the integration over $0 < v < \infty$ and $0 < w < \infty$ by an integration over $0 < \theta < \pi/2$ and $0 < r < \infty$

$$\text{i.e.} \int_0^\infty dw \int_0^\infty dv \frac{e^{-(u^2 + v^2 + w^2)^{\frac{1}{2}}}}{u^2 + v^2 + w^2} = \frac{\pi}{2}\int_a^\infty \frac{e^{-z}}{z}\,dz \tag{1.9}$$

and $$\psi = \frac{1}{\alpha}\int_0^\infty e^{-\frac{qx}{\alpha}}\,dx \int_x^\infty du \int_u^\infty \frac{e^{-z}\,dz}{z} \qquad (1.10)$$

which on reversing the order of integration of u and z becomes

$$\psi = \frac{1}{\alpha}\int_0^\infty dx\, e^{\frac{-qx}{\alpha}} \int_x^\infty \left[e^{-z}\left(\frac{z-x}{z}\right)dz\right] \qquad (1.11)$$

and on changing the order again

$$\psi = \frac{1}{\alpha}\int_0^\infty \frac{e^{-z\left(1+\frac{q}{\alpha}\right)}}{z}\,dz \int_0^z e^{\frac{q\theta}{\alpha}}\,d\theta \qquad (1.12)$$

where θ is a dummy variable.

Hence

$$\psi = \alpha \int_0^\infty \frac{e^{-z\left(1+\frac{q}{\alpha}\right)}}{z\,q^2}\left(1 + \frac{qz}{\alpha}e^{\frac{qz}{\alpha}} - e^{\frac{qz}{\alpha}}\right)dz$$

$$= \frac{1}{q} + \frac{\alpha}{q^2}\left[\int_0^\infty \frac{e^{-z\left(1+\frac{q}{\alpha}\right)}}{z}dz - \int_0^\infty \frac{e^{-z}}{z}\,dz\right]$$

After some rearrangement we obtain

$$\psi = \frac{1}{q} - \frac{\alpha}{q^2}\log_e\left(1+\frac{q}{\alpha}\right) \qquad (1.13)$$

3. Limiting forms of the ignition equations for large and small values of ha.

We consider equation (25) at the extreme values of ha. When $ha \to 0$, the first root of β tends to $\sqrt{3\,ha}$ and the first term on the right hand side tends to

$$\frac{2}{2+ha}\left[1 - \frac{\alpha R a P C}{3H}\log\left(1+\frac{3H}{\alpha R a P C}\right)\right]$$

The term $\frac{\alpha R a^2}{k\beta^2}$ may be written $\frac{\alpha R a P C}{H}\,\frac{ha}{\beta^2}$ so that if $\frac{\alpha R a P C}{H}$ is finite this term tends to zero as $ha \to 0$ and the term in brackets tends to unity and the remainder of the series tends to zero as $ha \to 0$.

i.e. $$\frac{H\,\theta_o}{I_m} = 1 - \frac{\alpha R\, a \rho C}{3H} \log_e \left(1 + \frac{3H}{\alpha R\, a \rho C}\right) + O(ha) \qquad (1.14)$$

For laminas and cylinders the result is the same when $\frac{a}{3}$ is replaced by the appropriate value of V/S. We thus obtain

$$\frac{H\,\theta_m}{I_m} = 1 - \frac{1}{g} \log_e (1 + g) \qquad (1.15)$$

where $g = \dfrac{S}{\alpha R V \rho C}$

When $ha \longrightarrow \infty$ the roots differ by π and $\beta = n\pi$ where $n = 1,2,3,4 \ldots$

$$\therefore \quad \frac{H\,\theta_o}{I_m} = 2\,ha \sum_0^\infty \frac{I_1 = \frac{R\,a^2 \alpha}{k\,n^2 \pi^2} \log \left(1 + \frac{k\,n^2 \pi^2}{R\,a^2 \alpha}\right)}{n^2 \pi^2 + (ha)^2 - ha} \qquad (1.16)$$

Only when n is of order ha do the terms in the series not remain of order $1/(ha)^2$. Let $n = \frac{y}{\pi}\,ha$ and disregard the first $\sqrt{ha}$ terms, whose sum is clearly less than $\frac{1}{\sqrt{ha}}$ and replace the series by $1/\pi$ of the integral viz:

$$\frac{H\,\theta_o}{I_m} = \frac{2}{\pi} \int_{\frac{1}{\sqrt{ha}}}^{\infty} \frac{1 - \frac{\alpha R}{k\,h^2 y^2} \log \left(1 + \frac{k\,h^2 y^2}{\alpha R}\right)}{y^2 + 1 + O\left(\frac{1}{\sqrt{ha}}\right)} \qquad (1.17)$$

The lower limit tends to zero as $ha \longrightarrow \infty$ and the integral can readily be reduced to

$$\frac{H\,\theta_o}{I_m} = 1 - \frac{2}{j} + \frac{2}{j^2} \log (1 + j) \qquad (1.18)$$

where $j = \dfrac{H}{\sqrt{\alpha R K \rho C}}$

A similar procedure derives equation (13) from equation (12).

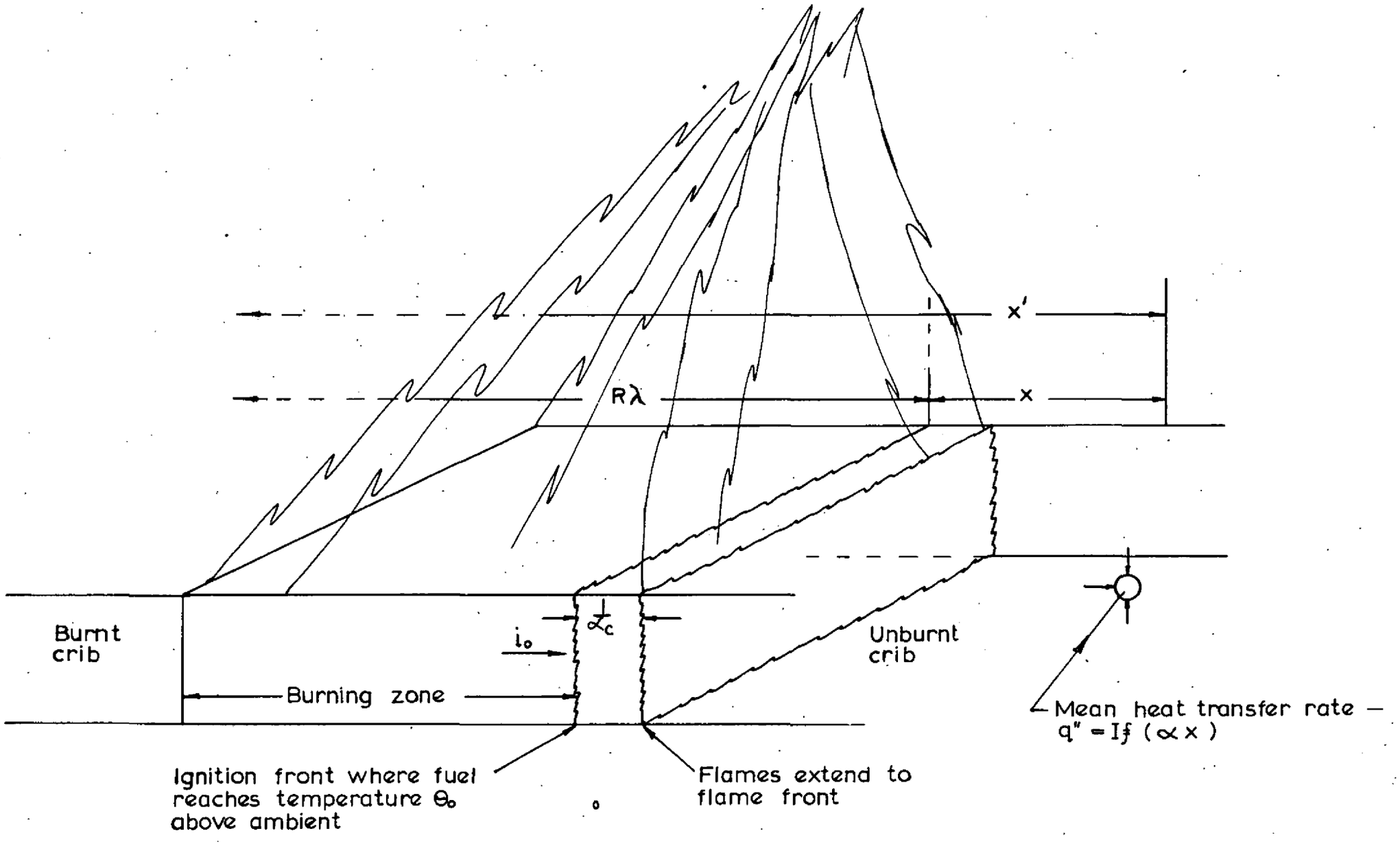

FIG.1. DIAGRAM OF FIRE SPREAD IN LONG BED OF FUEL

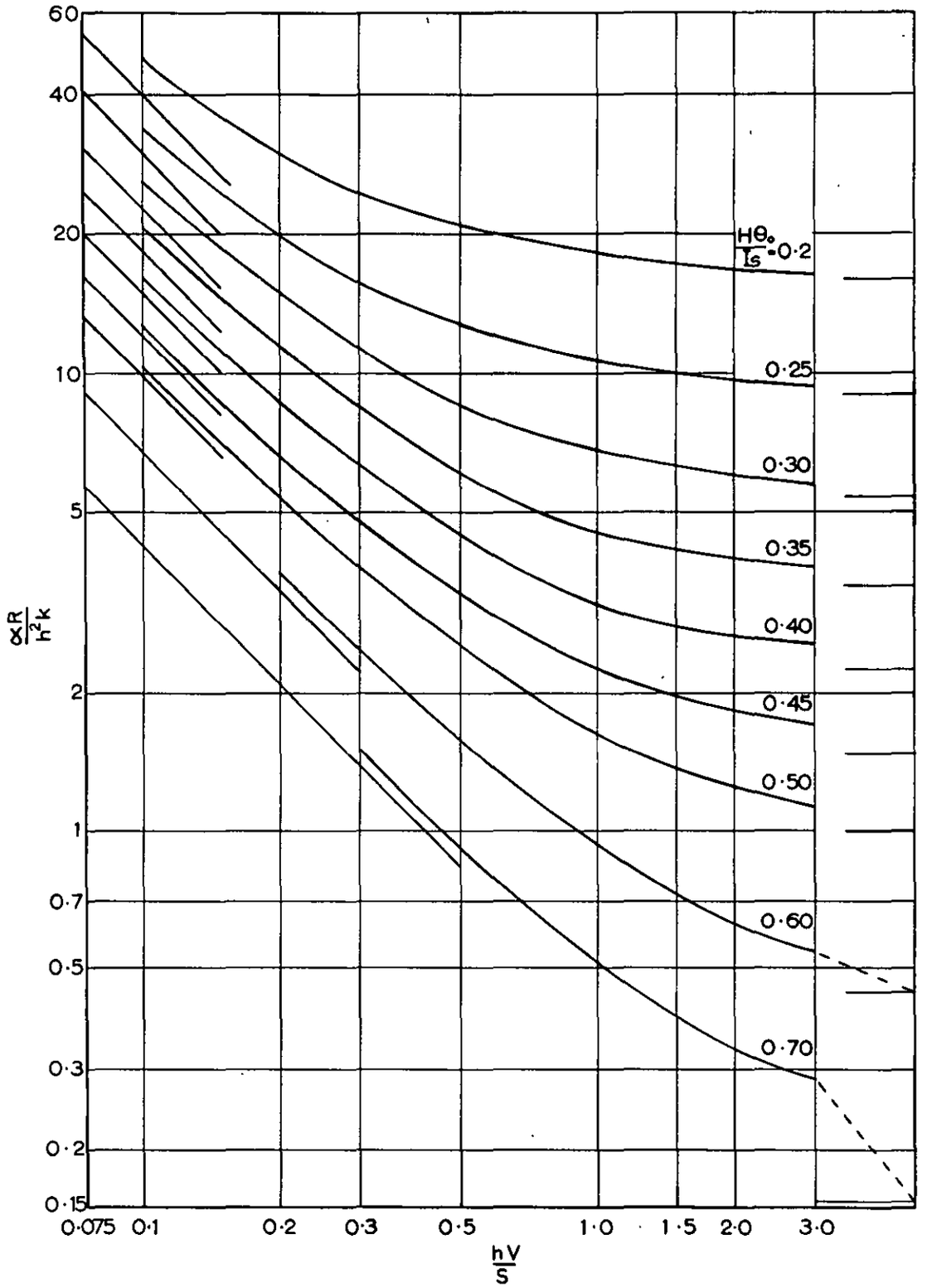

FIG. 2. CALCULATED PREHEATING RELATIONS (SINGLE RAY THEORY FOR CYLINDERS AND SPHERES)

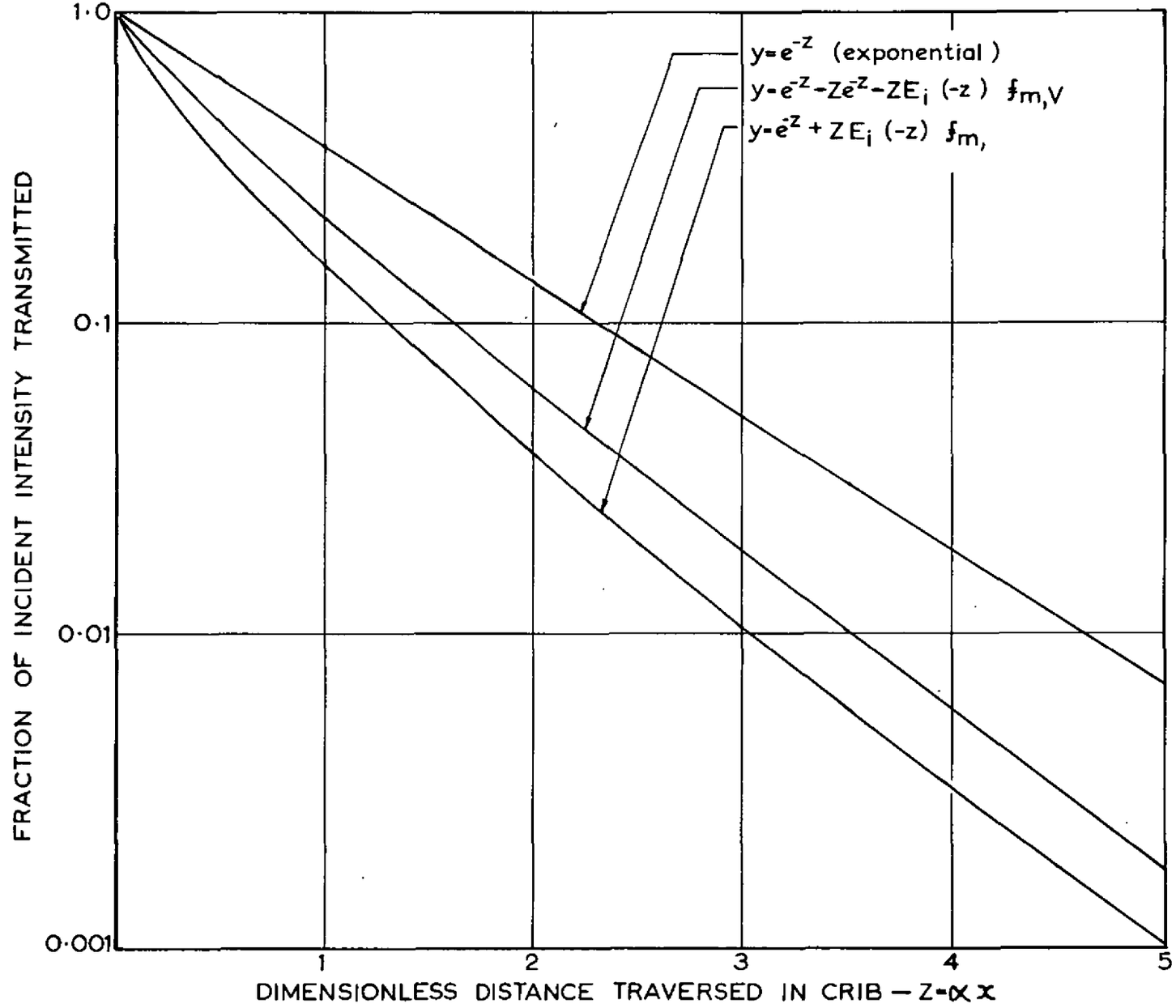

FIG. 3. THEORETICAL RELATIONS FOR ATTENUATION OF RADIATION

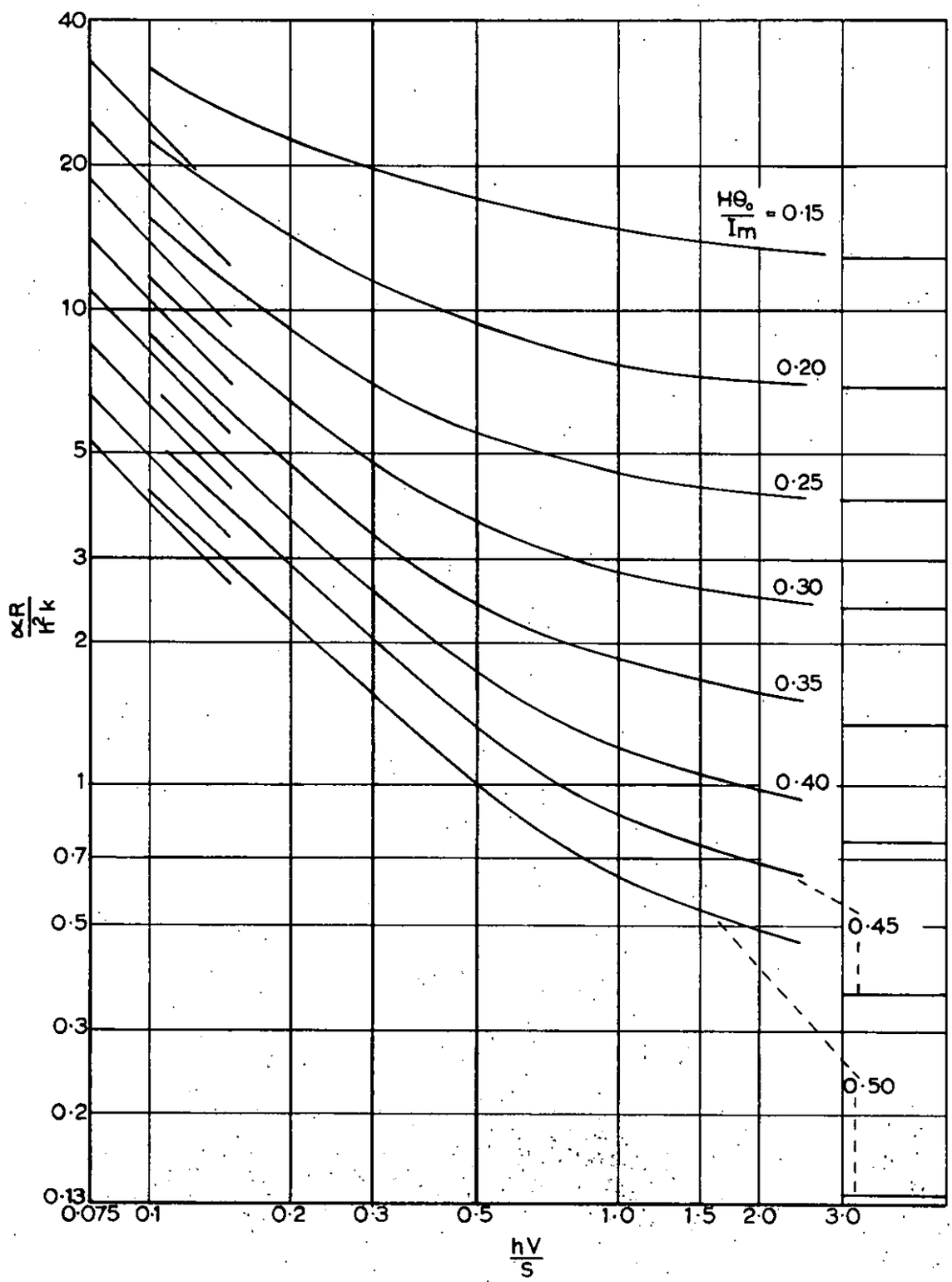

FIG. 4. CALCULATED PREHEATING RELATIONS (MULTIPLE RAY THEORY FOR CYLINDERS AND SPHERES)

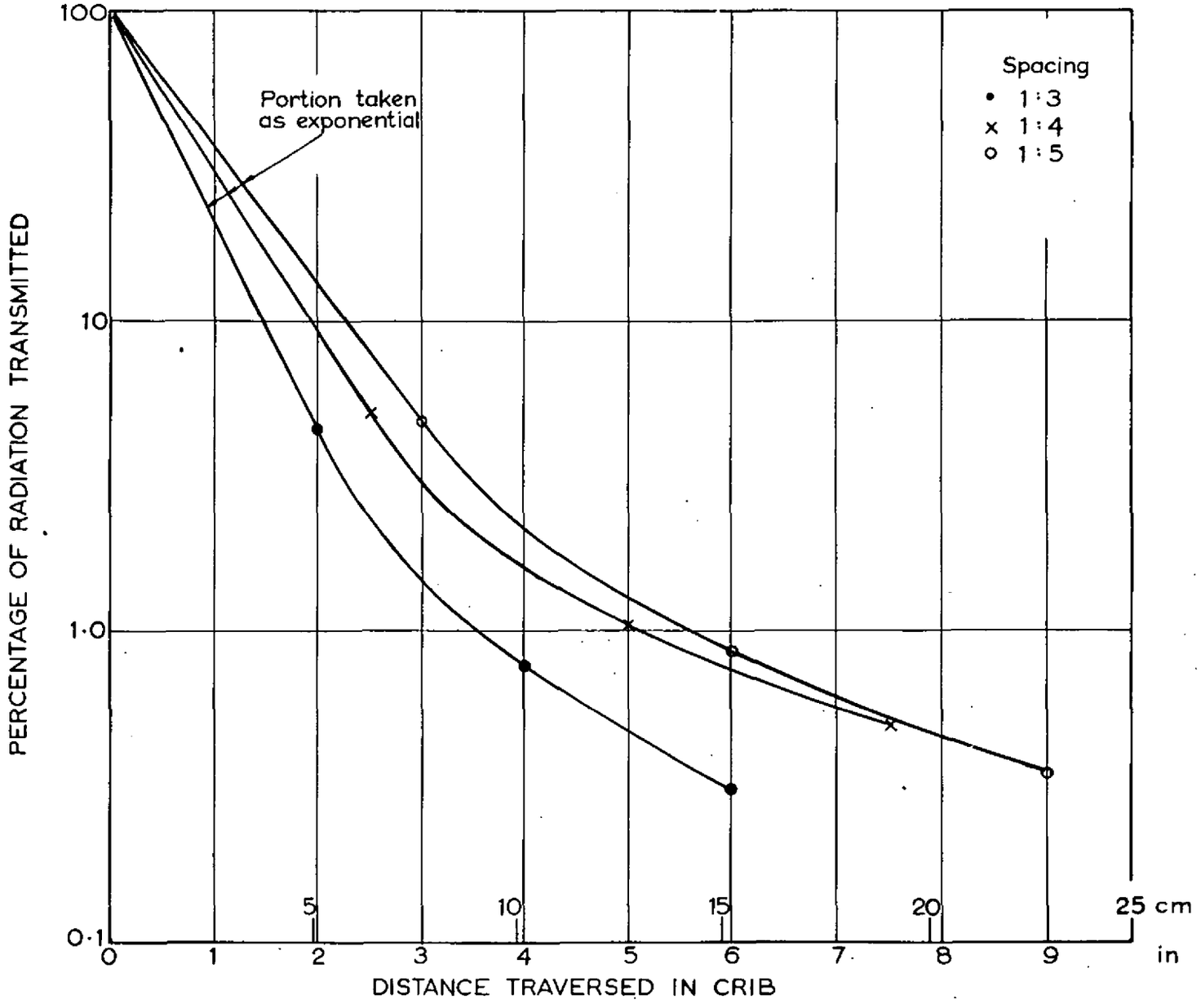

FIG. 5a. RADIATION TRANSMITTED THROUGH CRIB ON TO VERTICAL, TOP AND BOTTOM SURFACES

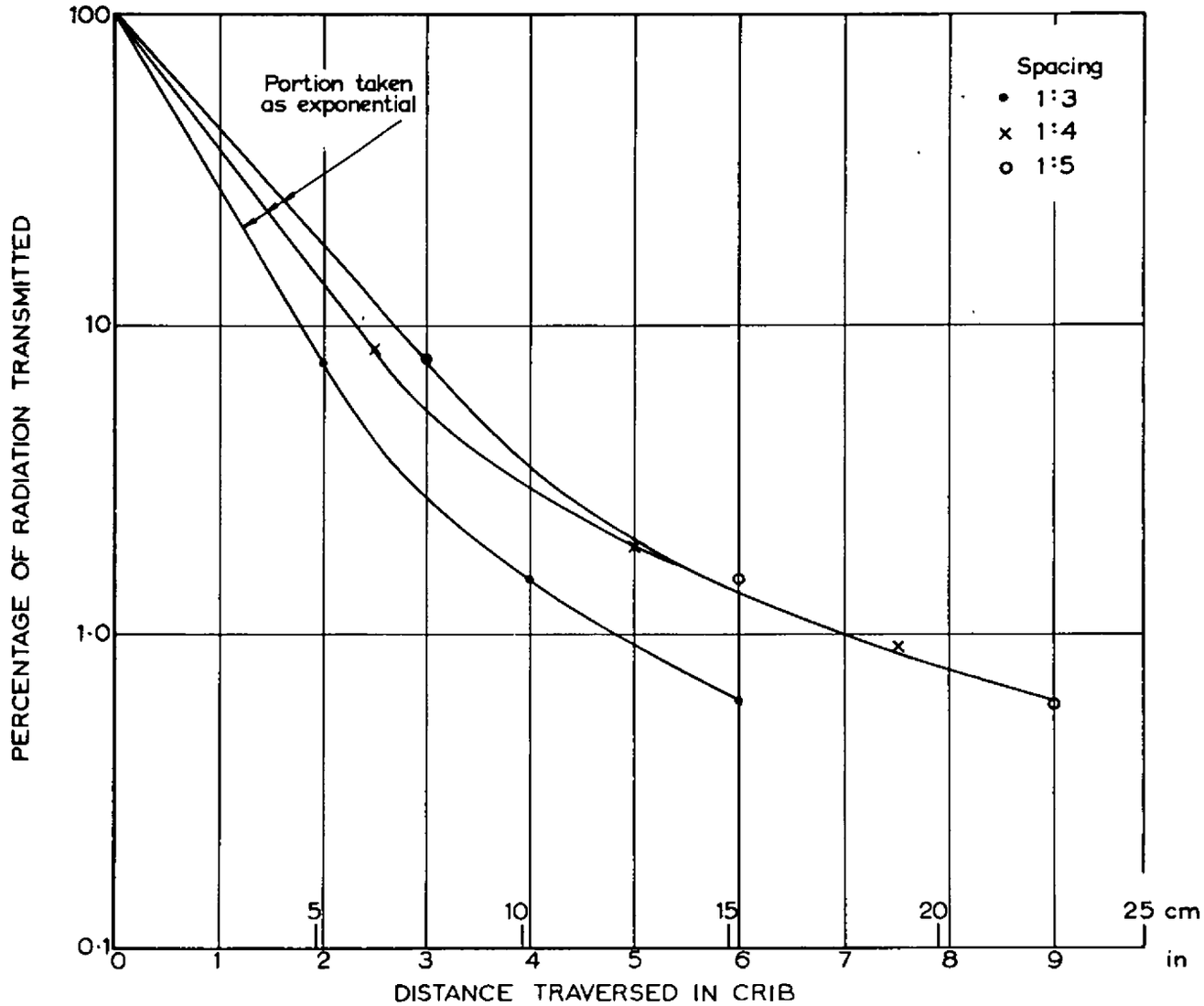

FIG. 5b. RADIATION TRANSMITTED THROUGH CRIB ON TO VERTICAL SURFACES

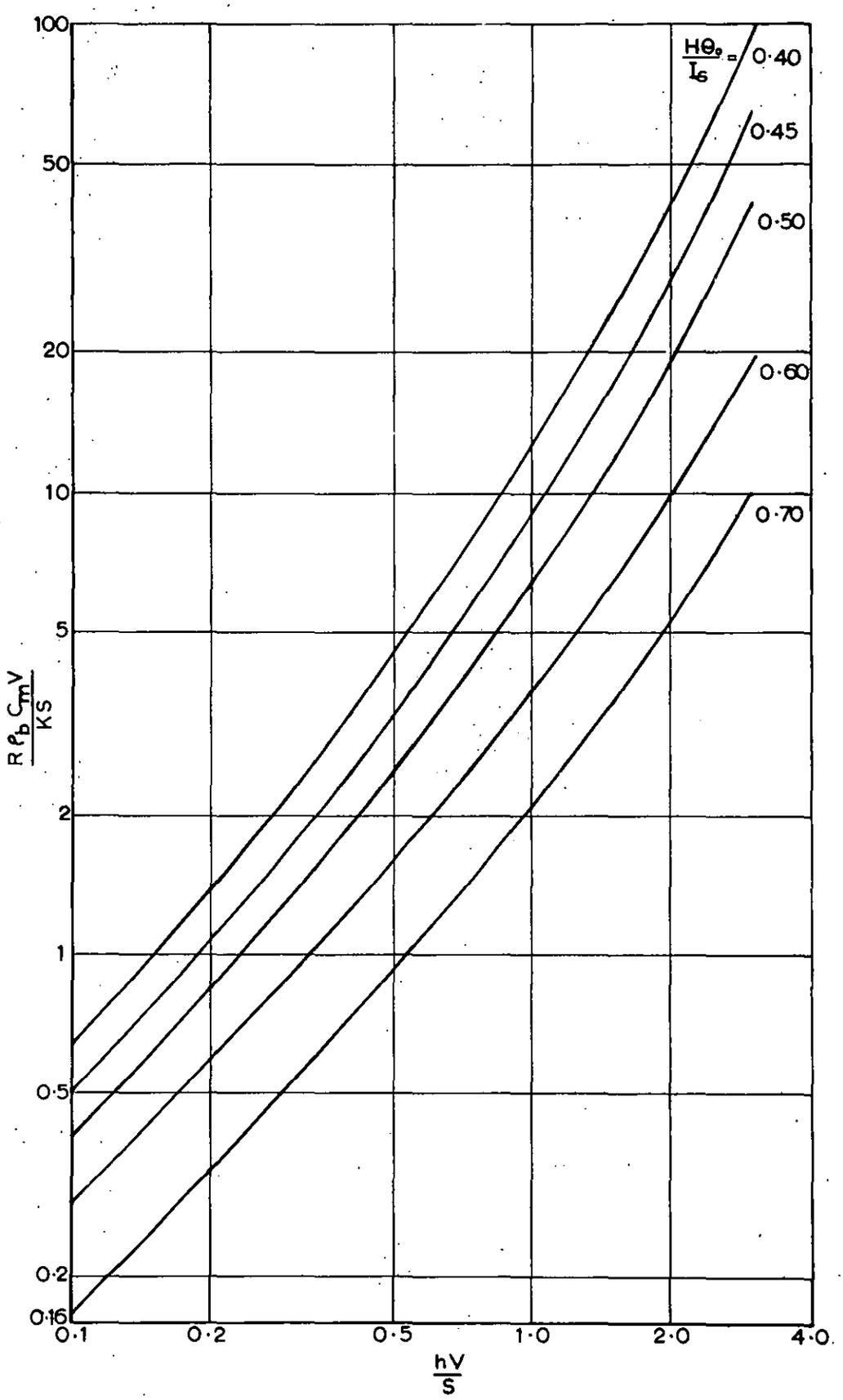

FIG. 6a. COMPUTED HEATING RELATIONS
(SINGLE RAY THEORY)

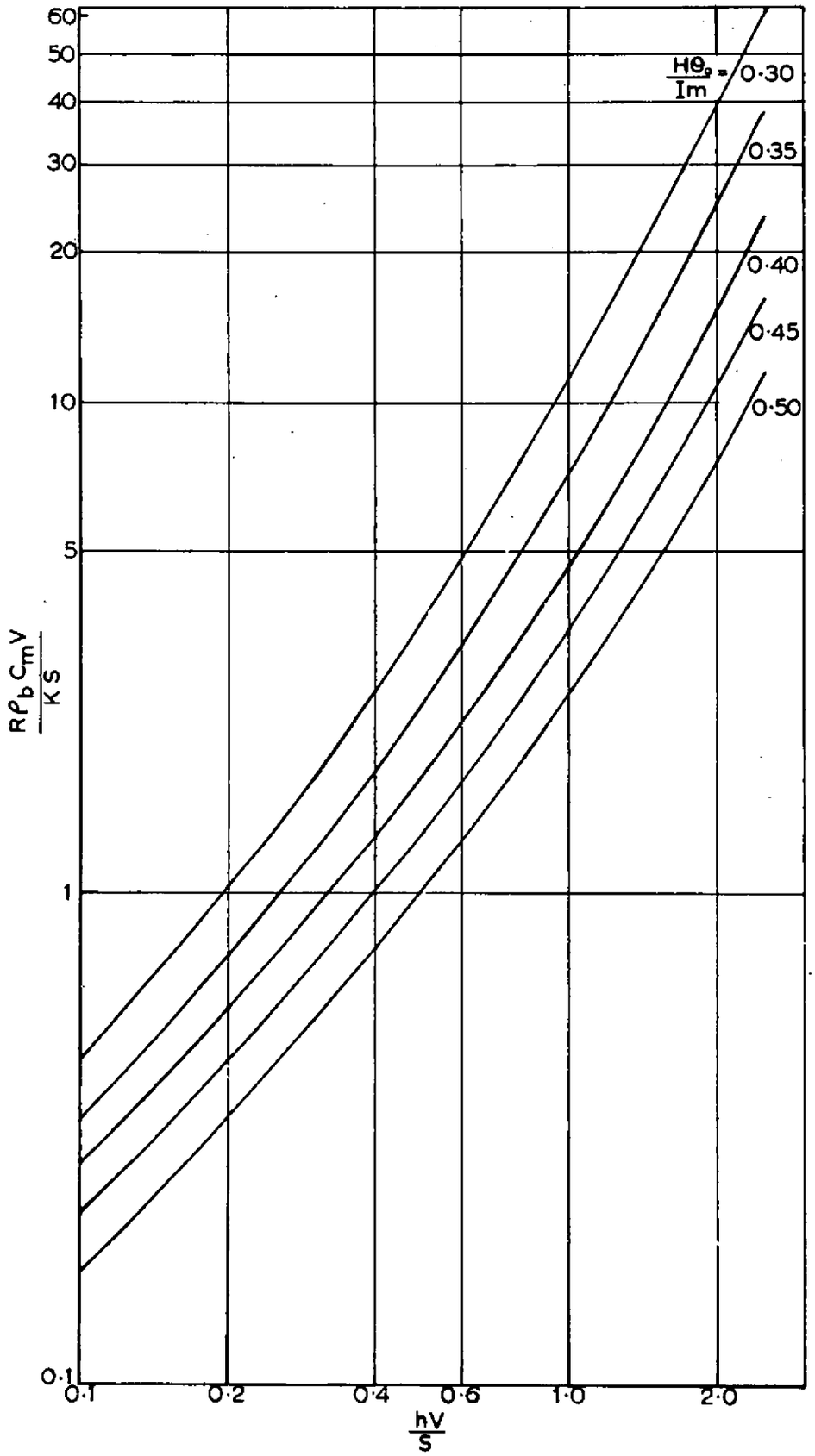

FIG. 6b. COMPUTED HEATING RELATIONS (MULTIPLE RAY THEORY)

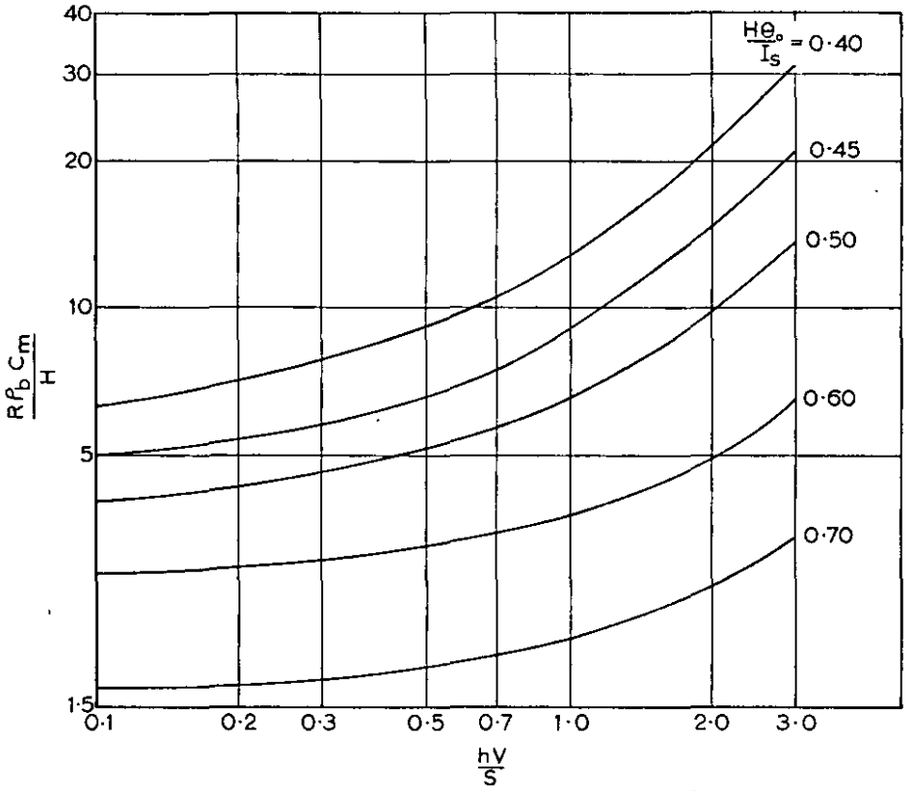

FIG.7a. COMPUTED HEATING RELATIONS
(SINGLE RAY THEORY)

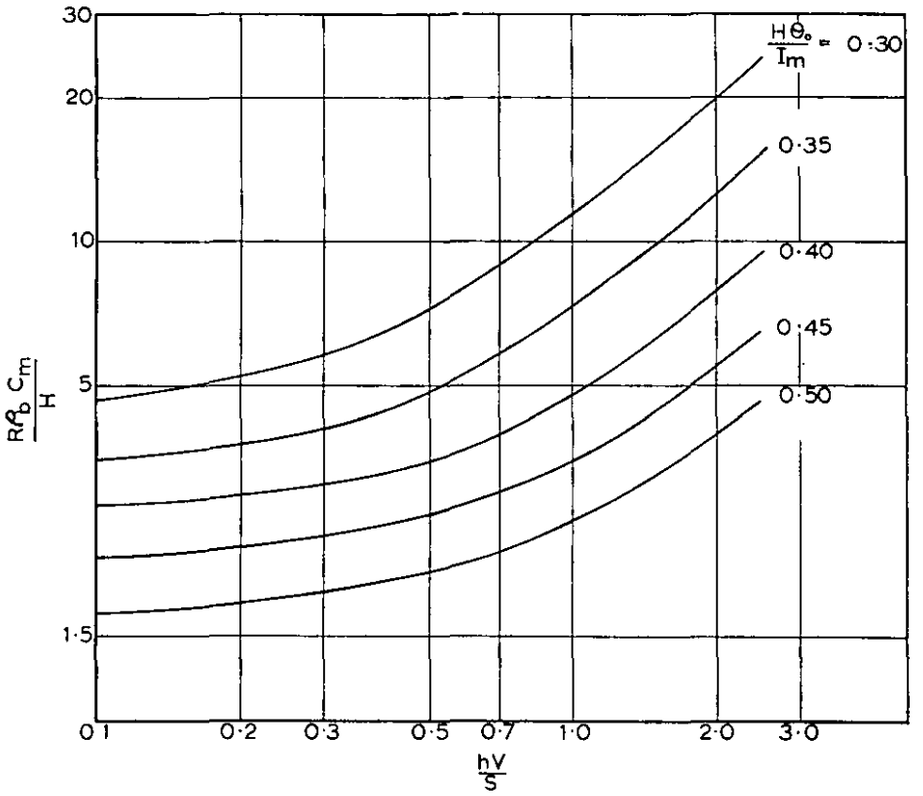

FIG.7b. COMPUTED HEATING RELATIONS
(MULTIPLE RAY THEORY)

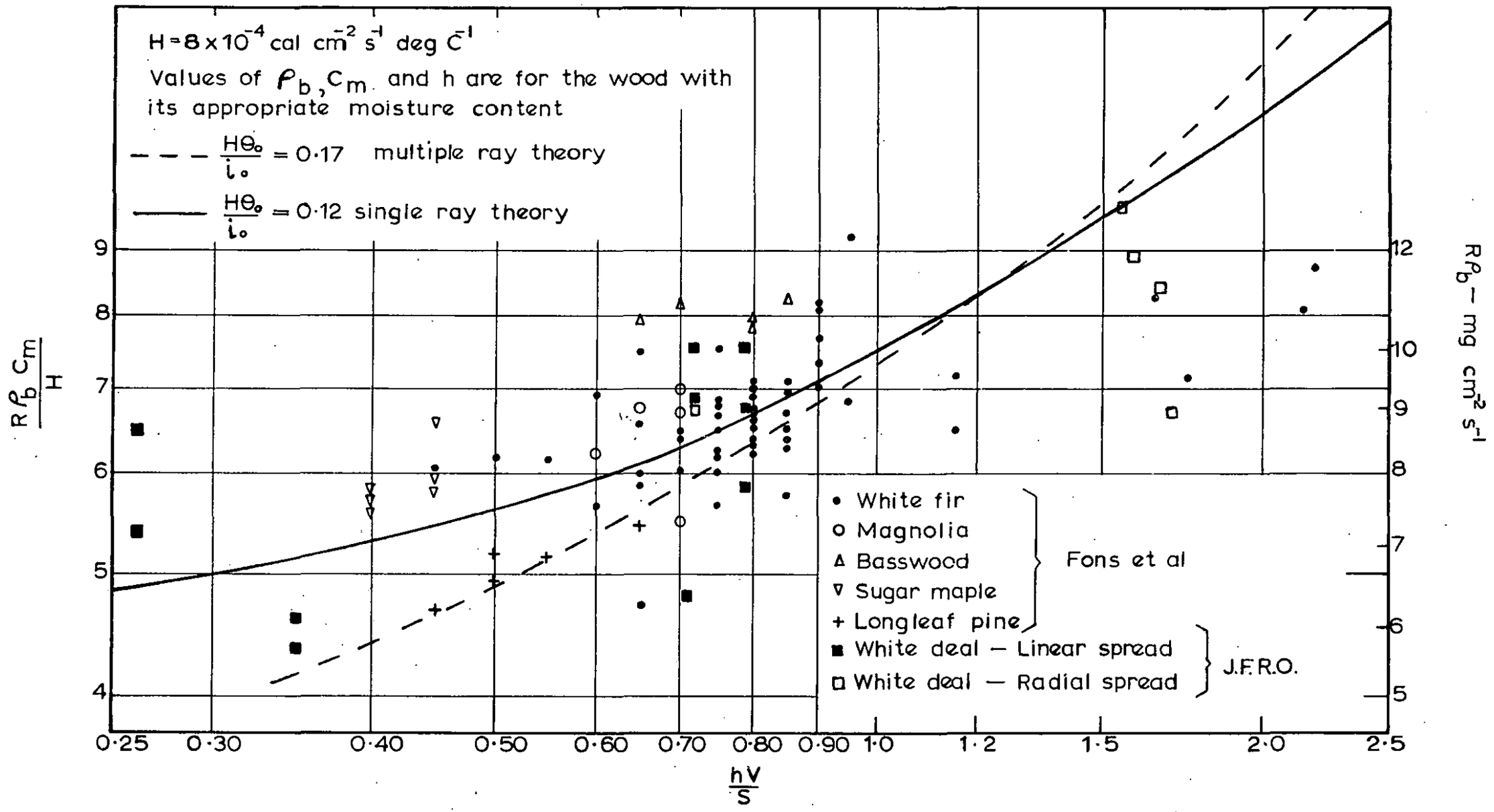

FIG.8a. RATE OF FIRE SPREAD IN CRIBS

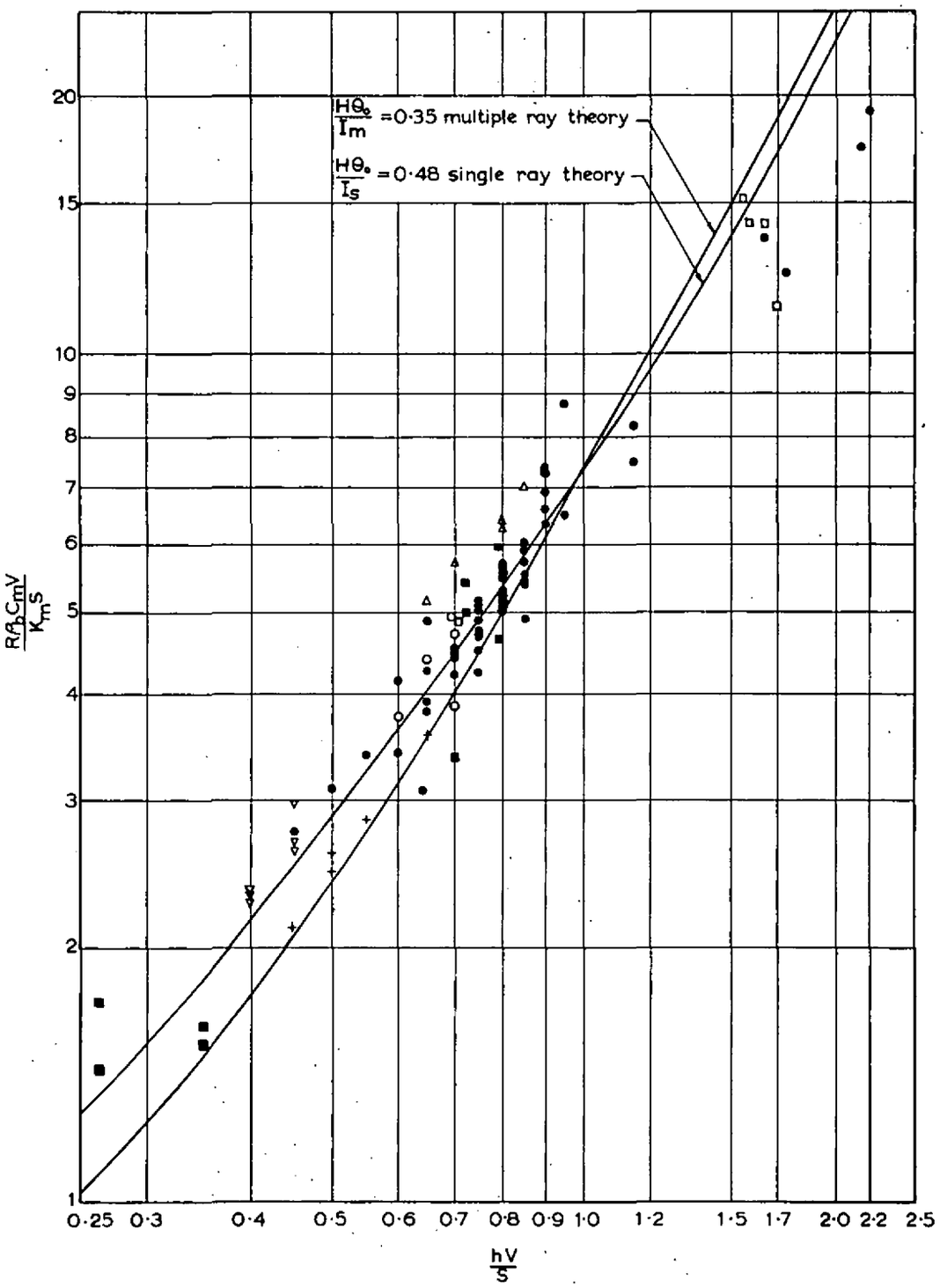

- ● White fir
- ○ Magnolia
- △ Basswood
- ▽ Sugar maple
- \+ Longleaf pine

} Fons et al

- ■ White deal – Linear spread
- □ White deal – Radial spread

} J.F.R.O.

Values of ρ_b, C_m, K_m and h are for the wood with its appropiate moisture content

FIG.8b. RATE OF FIRE SPREAD IN CRIBS

F.R.537
1/5414

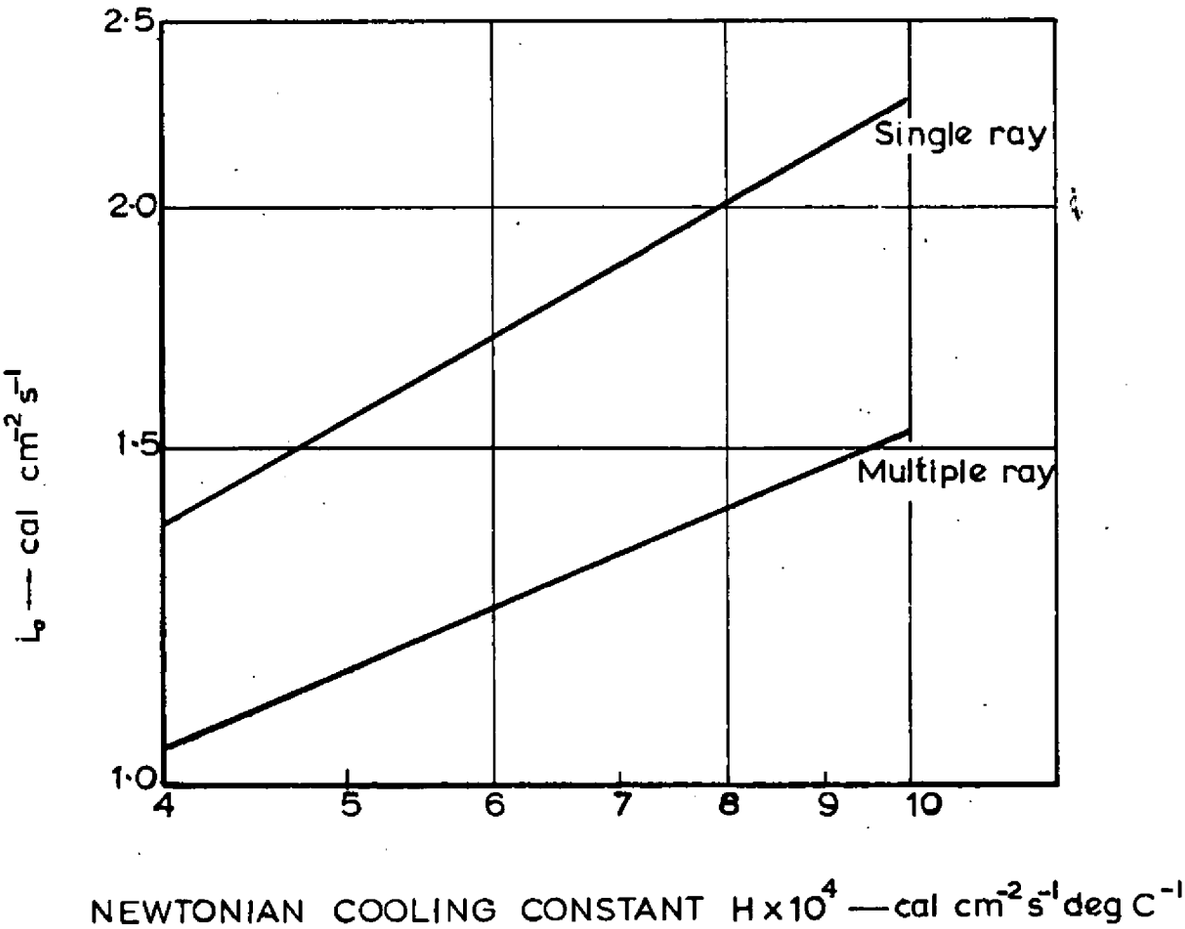

FIG. 9. ESTIMATE OF i_o FOR CRIB DATA